Natural Hazards (2022) 110:2163–2184
https://doi.org/10.1007/s11069-021-05029-5

ORIGINAL PAPER

Rapid changes to glaciers increased the outburst flood risk in Guangxieco Proglacial Lake in the Kangri Karpo Mountains, Southeast Qinghai-Tibetan Plateau

Yanjun Che[1,2,3,4] · Shijin Wang[1] · Yanqiang Wei[1] · Tao Pu[1] · Xinggang Ma[1]

Received: 7 April 2021 / Accepted: 9 September 2021 / Published online: 18 September 2021

Abstract

The Kangri Karpo Mountain Range on the Qinghai-Tibet Plateau frequently experiences glacial lake outburst floods (GLOFs). This study assessed the risk of outburst floods for Guangxieco Proglacial Lake (GPL) in this Mountain Range as a typical case to reveal the effects of rapid glacial change. The area of Gongzo Glacier behind GPL decreased by $7.39 \pm 0.10\%$ from 1987 to 2019, while this glacier advanced by 32.45 m from 5 June to 27 October in 1988. Guangxieco Proglacial Lake decreased from 0.42 ± 0.03 km^2 in 1987 to 0.19 ± 0.03 km^2 in 1988 and then continuously expanded to 0.43 ± 0.04 km^2 in 2019. Heavy precipitation occurred before 15 July 1988, when no supraglacial lake existed. Meanwhile, sustained abnormally high air temperature caused accelerated glacier and snow melting. Since 1988, a larger volume of rainfall and meltwater impounded by the ice wall caused an increase in the basal water pressure in the glacier. A significant increase in winter mass balance has caused a further increase in the downward gravity component of glacier sliding. As a result, the glacier advanced rapidly while reopening previously blocked subglacial drainage systems. The accumulating subglacial water rapidly drained into the Proglacial Lake causing an elevated lake level and a GLOF event. However, the current area of the glacial lake has recovered to the scale present before the outburst in 1988. Therefore, local government agencies and the local community should improve early warning systems and take measures designed to prevent a new GLOF and to minimize the risk of a recurrence of a GPL outburst.

✉ Yanjun Che
che_yanjun@126.com

✉ Shijin Wang
xiaohanjin@126.com

[1] Yulong Snow Mountain Glacier and Environment Observation and Research Station/State Key Laboratory of Cryospheric Sciences, Northwest Institute of Eco-Environment and Resources, Chinese Academy of Sciences, Lanzhou 730000, China

[2] Department of Geography Science, Yichun University, Yichun 336000, China

[3] Nanchang Base of International Centre on Space Technologies for Natural and Cultural Heritage under the Auspices of UNESCO, Nanchang 330000, China

[4] Key Laboratory of Poyang Lake Wetland and Watershed Research (Jiangxi Normal University), Ministry of Education, Nanchang 330000, China

Keywords GLOF · Glacier surge · Guangxueco Proglacial Lake · Qinghai-Tibetan Plateau

1 Introduction

Mountain glaciers worldwide have retreated extensively in recent decades due to climate warming, which is resulting in the formation and expansion of glacial lakes, increasing the potential risk of Glacial Lake Outburst Floods (GLOFs) (Shugar et al. 2020; Tiberti et al. 2020; Emmer and Vilímek 2013). When a glacier retreats, it may leave behind a large impression in the ground that fills with water, creating a lake. A Proglacial Lake has been defined as a moraine-dam glacial lake (Carrivick and Tweed 2013). Proglacial Lakes are widely distributed in many mountain ranges, such as the Hindu Kush, Karakoram, Himalayas, Nyainqentanglha, and Hengduan Shan (Veh et al. 2020; Ding et al. 2018; Imran and Ahmad 2021; Zheng et al. 2021). Glaciers are dynamic bodies of ice that change frequently; melting and the creation of dynamic features significantly affect the formation, expansion, and outburst of glacial lakes (Emmer and Cochachin 2013). A GLOF occurs when natural dam fails and meltwater is released from a moraine- or ice-dam glacial lake. When a moraine dam of a glacial lake fails, the water will burst out, potentially leading to massive floods and debris flows that may cause extensive damage downstream, including a loss of life and infrastructure (Grabs and Hanisch 1992). Alternatively, and more commonly, glacial ice from a retreating glacier or glacial advance (e.g., glacial surge) could crash into lakes, generating giant waves that can erode weak moraine dams in a matter of minutes, thereby also triggering GLOFs. Outbursts from lakes dammed by end moraines are closely associated with ice avalanches, and 79% of all dam failures occurred during July to August when ice avalanches occur frequently in mountain ranges of the Tibetan Plateau (Ding and Liu 2017).

Moraine-dammed lakes are impounded in between an end moraine complex and a vanishing glacier tongue, which creates a high probability of outburst due to commonly occurring ice avalanches, glacier surges, unconsolidated dam material, and unstable dam geometries, in rockfall- and landslides-prone areas or by earthquakes, and so on (Worni et al. 2012; McKillop and Clague 2007; Round et al. 2017). These volatile lakes form when glaciers disappear making it more likely that downstream communities may experience flash floods, landslides, and other calamities as a result. These GLOF disasters (GLOFDs) can occur in many parts of the world where people live downstream from these hazardous glacial lakes, mostly in the Andes and in places such as Bhutan and Nepal, where these floods can be devastating (Veh et al. 2020; Zhang et al. 2020). Many GLOFDs have been frequently observed, recorded, or reported in the Himalayas, Peruvian Andes (Cordillera Blanca), Chile's Patagonia, the Canadian Rockies, on the Southeastern Qinghai-Tibetan Plateau (QTP), and elsewhere (Wang et al. 2015; Zheng et al. 2021). For example, at least 20 GLOFDs have occurred in the southeastern QTP since 1935 such as the outburst of Guangxieco Proglacial Lake (GPL), which occurred suddenly at 23:30 (China, UTC + 8) on July 15,1988. This GLOFD caused a blockage for half an hour, which then triggered secondary disasters caused by a dam break. Secondary disasters flash floods along the Parlung Zangbo River washed away 18 bridges, severely destroying 42 km of the Sichuan-Tibet Highway, and causing traffic disruption for six months, with a total economic cost estimated at over CNY 100 million (Lv et al. 1999; Liu et al. 2014; Li and You 1992).

Most lake-terminating mountain glaciers have retreated rapidly due to the periodic loss of frontal ice loss at their termini, but long-term observations were limited regarding their

flow and melt dynamics, which are crucial to understanding the processes of ice mass loss and Proglacial Lake growth (Liu et al. 2020). As glaciers continue to retreat and feed glacial lakes with increasing amounts of glacier melt, the implications for GLOFs and water resources are of considerable societal and ecological importance. The potential risks of GLOFs and GLOFDs have been increasing under the background of local climatic warming. The present study is focused on the changes of Gongzo Glacier and the GLOF of GPL in the Kangri Karpo Mountains of the southeastern QTP. The goal was to (I) assess the changes of Gongzo Glacier during the past several decades; (II) understand the expansion of the GPL and evolution of supraglacial lakes on this glacier; (III) discuss the cause of the GPL's GLOF event in 1988. In addition, we re-assessed the outburst potential risk of GPL and provide basic database and technical support for GLOF disaster prevention and reduction in the southeast region of the QTP.

2 Study area

Gongzo Glacier, also called Midui Glacier, is located at 29.41°N, 96.51°E in the Kangri Karpo Mountain Range in the southeast QTP (Fig. 1). Guangxieco Proglacial Lake formed 300 years ago (Li and You 1992) and was mainly fed by the meltwater for Gongzo Glacier. The glacier is coded as 5O282B0083 in the Chinese Glacier Inventory; its meltwater ultimately flows into Parlung Zangbo River. In contrast with other places on the QTP, this region experiences strong seismic activity, heavy precipitation, and warm ice temperatures (Wu et al. 2018). The glacier is a maritime temperate glacier with an area of ~ 29 km^2 and length of ~ 10 km. Glacier surface elevation ranged from 6293.40 to 3848.10 m a.s.l., corresponding the glacier flow from south to north (Liu et al. 2015). The glacier has western and eastern tributaries, with their firm snow zone distributed above the elevation of 4850 m

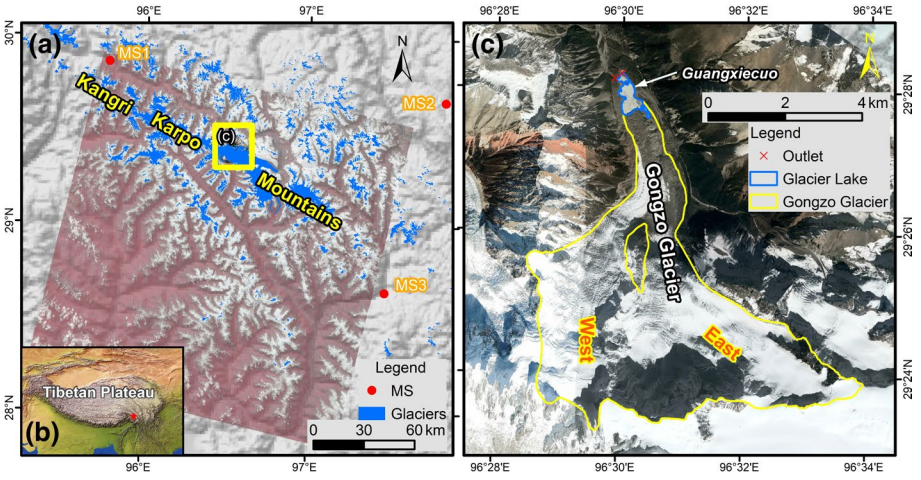

Fig. 1 Guangxieco Proglacial Lake and Gongzo Glacier in the study area. (a) A red rectangle denotes the LandSat Image range of a scene covering Gongzo Glacier. The three closest Meteorological Stations (MSs) are Bomi MS (MS1), Zogang MS (MS2), and Zayü MS (MS3) with MS1 closest to Gongzo Glacier. (b) Spatial position of the study region in the Qinghai-Tibetan Plateau. (c) Topography of the glacier and glacial lake. The glacier is oriented from south to north, and glacier tongue faces to the north. The glacier terminus is inserted into Guangxieco Proglacial Lake

a.s.l. Ice cliffs were previously located between 4850 and 4100 a.s.l. with a glacier slope of 25°–30° (Li and You 1992). In addition, the glacier tongue, i.e., ablation zone, was covered by debris with a thickness of > 50 cm.

A moraine-dammed lake, specifically GPL, formed when the one terminal moraine acted as a barrier to the flow of meltwater originating from Gongzo Glacier (Li and You 1992). Before 1988, two outlets on the dam of terminal moraine were in the north terminus of the lake, located in the northwestern and northeastern parts of the dam (Fig. 1). The glacial lake was recharged by precipitation and meltwater from Gongzo Glacier, and the front of the tongue of Gongzo Glacier extended into the lake. The eastern part of the lateral moraine had a relatively steep slope with loose rock and fragments frequently falling as talus, while many trees grew on the west lateral moraine (Fig. 1c).

3 Data and methods

3.1 Remote sensing images

To understand the changes of Gongzo Glacier and GPL, some open-access orthorectified LandSat Thematic Mapper (TM), Enhanced Thematic Mapper (ETM +), Operational Land Imager (OLI), and Google Earth images were obtained. Spatial ranges of the glacier and Proglacial Lake were mainly derived from LandSat images. For the LandSat multiband images, the spectral-band ratio method has been demonstrated to be a simple, highly efficient, and accurate technique that can be used to extract the outline of glaciers (Silverio and Jaquet 2005; Sidjak 1999). This method can reduce the errors caused by sensor saturation and shadowed areas, and can discriminate debris-mantled ice and ice-marginal water bodies (Paul et al. 2004). Based on the assessed experience of glacier change in Yulong Snow Mountain (Wang et al. 2020), we first used the spectral red-band and short-wave infrared-1 (SWIR1-band) methods to calculate the band ratio (i.e., TM3/TM5 for TM and ETM +, TM4/TM6 for OLI) (Mölg et al. 2018; Paul et al. 2002). Next, we manually traced the outlines of the glacier and Proglacial Lake boundaries for each year in the region and modified the outline by manual visual interpretation. In addition, the images provided by Google Earth were applied as the reference for the glacier and Proglacial Lake outlines, which were also used to understand the formation and disappearance of the proglacial and supraglacial lakes. Detailed information about the dataset of remote sensing images used in this study is given in Table 1.

Radar satellites are critical to our understanding of the changes in surface elevation change of Gongzo Glacier due to the lack of a ground observation dataset. To assess the changes in surface elevation and mass balance in glaciers globally, Hugonnet et al. (2021) produced datasets that provide glacier surface elevations globally since 2000. They retrieved all data related to and intersecting glaciers worldwide including data from the advanced spaceborne thermal emission and reflection radiometer, ArcticDEM, and the Reference Elevation Model of Antarctica (REMA) data. Meanwhile, TerraSAR-X add-on for Digital Elevation Measurement (TanDEM-X) satellite data was used as a globally homogeneous reference for co-registration and bias correction over ice-free terrain, keeping only elevations with an error smaller than 0.5 m in the provided TanDEM-X height error map. In addition, Shuttle Radar Topography Mission (SRTM) digital elevation model (DEM) data acquired in February 2000 were referenced as a database of a time series of the initial changes in glacier surface elevation in the study area. In this paper, the surface elevation

Table 1 Information of remote sensing images used in this study

	Path/Row	Date	Bands	Resolutions (m)
LandSat8	134/40	2019/11/02	Bands 5/4/3	30
		2017/06/05	Bands 5/4/3	30
		2013/09/14	Bands 5/4/3	30
LandSat7	134/40	2009/09/27	Bands 4/3/2	30
		2006/09/19	Bands 4/3/2	30
LandSat5	134/40	2000/05/05	Bands 4/3/2	30
		1995/10/15	Bands 4/3/2	30
		1988/10/27	Bands 4/3/2	30
		1988/06/05	Bands 4/3/2	30
		1987/12/28	Bands 4/3/2	30
Google Earth		2017/11/18	–	
		2014/11/08	–	
		2001/11/14	–	

data for the Gongzo Glacier from 2000 to 2019 were retrieved from a dataset of glacier time series on the website of https://doi.org/10.6096/13. The changes in elevation of the glacier surface were converted to mass balance changes using an ice density of 900 kg/m^3.

3.2 Methods of estimating changes in glacier area, volume, and length

Previous researchers have used the Annual Percentage of Area Changes (APAC) to understand the changes to the spatial extent of glaciers in different periods (Ding et al. 2006; Xu et al. 2015; Che et al. 2018; Wang et al. 2011), which is calculated using Eq. (1):

$$\mathrm{APAC} = \frac{\Delta S}{S_1 \Delta t} \tag{1}$$

where APAC is the annual percentage of a change in area, S_1 is the area of the glacier at the initial time, $\Delta S = S_2 - S_1$ is the change in area of the glacier during the study period, S_2 is the area of the glacier at the last time measured, and Δt is the time span of the change in the glacier during the past several years. In addition, the glacier length was manually interpreted along with a center line of the glacier flow path. We interpreted two center lines per year of the main stream on the glacier surface, i.e., the west and east glacier length. The spatial analysis tool of ArcGIS software was used to calculate the glacier area and length.

3.3 Glacial lake capacity

The calculation of the capacity of moraine-dammed glacial lake reservoirs is one of the important parameters used for estimating the peak discharge of a glacial lake outburst and understanding the process of GLOF (Ng et al. 2007). An empirical statistical model was developed based on the *in situ* dataset of Longbasaba Proglacial Lake on the north slope of the Himalayas to calculate the capacity of the glacial lake, as shown in Eq. (2) (Yao et al. 2010):

$$V = 0.0493\mathrm{A}^{0.9304} \tag{2}$$

where V is the reservoir capacity of a glacial lake (unit km^3) and A is the area of the glacial lake (km^2). In this study, the capacities of the glacial lakes were assessed using this equation.

3.4 Glacier mass balance

The mass balance of a glacier is the difference between ice accumulation and ablation over a specific period, which is a key factor to understanding the fluctuations in regional climate and glacier runoff (Cogley 2009; Andreassen et al. 2016). However, no observational data for mass balance of Gongzo Glacier were available. To fill this gap, we used a Degree-Day Model (DDM) to simulate the mass changes in Gongzo Glacier. Researchers have often used DDMs to understand the glacier mass balance dynamics due to their use of simple input data and good performance (Kääb et al. 2018; Gilbert et al. 2016). Degree Day Factors (DDFs) related to ice and snow were crucial to the DDM simulation. In general, a DDF represents a discrepancy between different types of glaciers. Maritime glaciers are likely to have higher DDFs than subcontinental and extremely continental glaciers; for example, the average values of DDFs for maritime, subcontinental, and extremely continental glaciers were 10.9, 7.2, and 4.3 mm d^{-1} $°C^{-1}$, respectively (Zhang et al. 2017). After repeated simulation and calibration for the DDM, a DDF for ice of 9.0 mm d^{-1} $°C^{-1}$ and a DDF for snow of 5.9 mm d^{-1} $°C^{-1}$ were finally used to simulate the glacier melting in this paper, respectively. The mass balance equation for glacier melting is given in Eq. (3):

$$M = \mathrm{DDF}_{\mathrm{ice/snow}} \times \mathrm{PDD} \tag{3}$$

where DDF is the degree-day factor, which is different for snow and ice. The PDD value (in °C d^{-1}) is defined as the excess of daily surface air temperature above the melting point accumulated over a balance year and M is the depth of meltwater in a specific period.

The accumulation of ice in a glacier generally depends on the snowfall, which is mainly controlled by the threshold of air temperature, ranging from 0 °C to 5.5 °C (Ding et al. 2014). An air temperature threshold of 3 °C is often used to define the precipitation as falling as snowfall in the study region (Ding et al. 2014). The lapse rate of 0.60 °C per 100 m was used to calculate the daily air temperature from Bomi meteorological station to the glacier surface. In addition, the SRTM DEM in the glacier region was used in the distributed model of glacier melt and accumulation. Herein, the glacier mass balance is given by Eq. (4):

$$B = \int_{t0}^{t1} (A - M)dt \tag{4}$$

where A and M are the glacier accumulation and ablation, respectively, and B is the mass balance over one year more generally over the period from t_0 to t_1.

3.5 Meteorological dataset

Meteorological records of three stations, including Bomi, Zogang, and Zayü meteorological stations, were used in this study to understand the changing climate of the region

(Table 2). Bomi station is located ~ 86 km northwest of Gongzo Glacier and has recorded data since 1955. Note that the records of air temperature and precipitation data from this station that were used in this study were acquired since 1960. Zogang and Zayü stations are located ~ 130 km northeast and ~ 127 km southeast of the glacier, respectively (Fig. 1). These two stations have recorded the local weather conditions since 1978 and 1969, respectively. These three meteorological stations were installed by the China Meteorological Administration, which provided the related datasets at http://data.cma.cn/. The periods of accumulation (September to April) and ablation (May to August) were used to describe the change of one hydrological period; therefore, the period of September to next August was also regarded as one year when analyzing the glacier mass balance.

3.6 Uncertainty and accuracy of Landsat image processing

In the past, the accuracy of the extracted glacier and glacial lake information has often been determined based on image quality, pixel resolution, radiometric and geometric corrections, threshold value selection, and expert experience (Hall et al. 2003; Salerno et al. 2012; Wang et al. 2017). The method proposed by Hanshaw and Bookhagen (2014) was used to calculate glacier and glacial lake area uncertainties in this paper. It assumed that the error was associated with area measurement and showed a normal or Gaussian distribution. Thus, we first calculated the number of pixels comprising the area measurement outline, using the perimeter divided by the grid cell size. The number of outline pixels was multiplied by 0.6872 ($\pm 1\sigma$), using the assumption that ~69% of the pixels are subject to errors. Finally, this figure was multiplied by half the area of a single pixel, assuming that the uncertainty for each pixel was half a pixel, using Eq. (5):

$$\text{Error}(1\delta) = (P/G)0.6872G^2/2 \tag{5}$$

where P is the glacier or glacial lake perimeter, G is the image spatial resolution and σ is the variance.

To reduce additional errors as much as possible, a more human-interactive examination was used for each Landsat image false-color composite, in conjunction with high-resolution Google Earth historic imagery.

4 Results

4.1 Changes in the area and length of Gongzo Glacier

The spatial extent of Gongzo Glacier increased by 0.41 km^2 from 1987 to 1988; however, this figure decreased continuously until 2019. During the periods of 2006–2009 and 2017–2019, the glacier presented higher APACs than during other time-spans,

Table 2 Information of meteorological stations (MSs) near Gongzo Glacier

Code	Name	Longitude	Latitude	Elevation	Time-span
MS1	Bomi	95.77	29.87	2736	1955–2019
MS2	Zogang	97.83	29.67	3780	1978–2019
MS3	Zayü	97.47	28.65	2327.6	1969–2019

including APACs of $-14.33 \pm 1.04\%$ and $-23.50 \pm 1.52\%$, respectively. In addition, the spatial extent of the glacier declined by 0.47 km^2 for 2017–2019, and the speed of the retreat speed was the highest among all time-spans from 1987 to 2019 with an APAC of $23.5 \pm 1.52\%$. The glacier area shrank from 31.44 ± 0.32 km^2 in 1988 to 29.15 ± 0.33 km^2 in 2019 with a rate of decrease of $7.39 \pm 0.10\%$ annually. Note that the glacier front advanced from 1988 to 1995, while the spatial extent of the glacier decreased slightly by 0.35 km^2. This phenomenon was mainly a result of glacial melting in several zones, e.g., the hill between the East and West branches of the glacier, and the debris-covered eastern terminus of glacier; these areas were located in relatively flat regions and were prone to obtaining relatively intense solar radiation (Fig. 2a and Table 3). In other words, the spatial extent of the glacier decreased by 1.88 km^2 from 1987 to 2019, with an APAC of $5.70 \pm 0.03\%$.

Gongzo Glacier retreated significantly during the period from 1987 to 2019 (Fig. 2). However, the glacier advanced from 1987 to 1995, during which glacier lengths increased from 10.81 km to 10.90 km in East branch and from 8.36 km to 8.45 km in the West branch. Here, the length of the East branch glacier was regarded as the length of the Gongzo Glacier in order to compare the time series in this paper. The glacier front advanced by 90 m from 1987 to 1995, with an advance of 30 m for 1987–1988 and 60 m for 1988–1995 (i.e., advance of 8.57 m/a). In addition, the glacier length decreased from 10.90 km in 1995 to 10.55 km in 2019. The annual length change of Gongzo Glacier was relatively small for 1995–2009, such as the annual length changes of -6.00 m/a for 1995–2000, -11.67 m/a for 2000–2006, and -6.67 m/a for 2006–2009. However, the retreat trend accelerated after 2009, i.e., the glacier averaged a retreat of 15 m/a for 2009–2013, 25 m/a for 2013–2017, and 35 m/a for 2017–2019. That is, the glacier front retreat accelerated significantly during the past decade. The glacier retreated by 260 m during the period of 1987–2019 with an annual retreat distance of 7.88 m/a, which resulted in a spatial expansion of 260 m along with the direction of glacial retreat (Fig. 2b–c and Table 3).

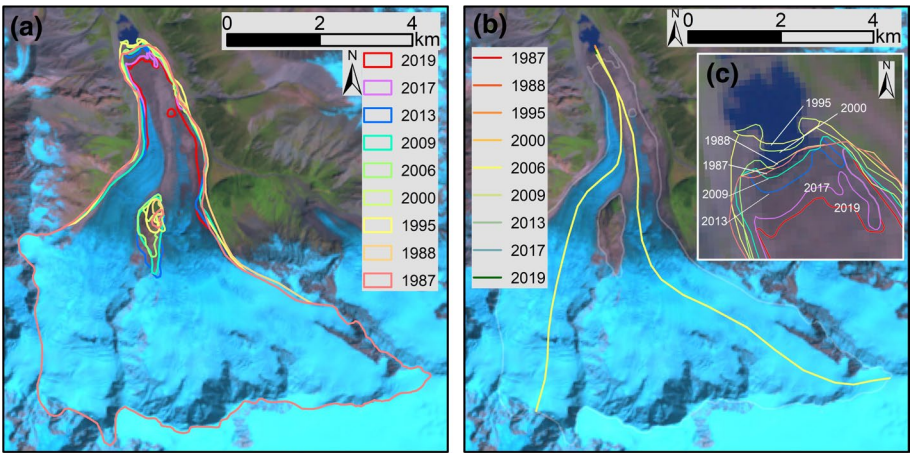

Fig. 2 Changes in the spatial extent and length of Gongzo Glacier from 1987 to 2019. The base image is a LandSat Image acquired in 2006. (a) Areal changes of Gongzo Glacier from 1987 to 2019. (b) Changes in the length of the glacier in the study period. (c) Changes in the glacial terminus from 1987 to 2019

Table 3 Changes in area and length of Gongzo Glacier

Year	Length		Advance/Retreat distance (m)	Annual front change (m)	Glacier area ± 1σ (km^2)	APAC (%)
	East branch	West branch				
1987	10.81	8.36	–	–	31.03 ± 0.32	–
1988	10.84	8.38	0.03	30.00	31.44 ± 0.32	41 ± 3.12
1995	10.90	8.45	0.06	8.57	31.09 ± 0.32	− 5 ± 0.45
2000	10.87	8.42	− 0.03	− 6.00	30.91 ± 0.33	− 3.6 ± 0.63
2006	10.80	8.35	− 0.07	− 11.67	30.60 ± 0.32	− 5.12 ± 0.51
2009	10.78	8.32	− 0.02	− 6.67	30.17 ± 0.32	− 14.33 ± 1.04
2013	10.72	8.26	− 0.06	− 15.00	29.79 ± 0.33	− 9.5 ± 0.78
2017	10.62	8.17	− 0.10	− 25.00	29.62 ± 0.33	− 4.25 ± 0.78
2019	10.55	8.09	− 0.07	− 35.00	29.15 ± 0.33	− 23.5 ± 1.52

APAC annual percentage of area changes

4.2 Glacial lake evolution

The Proglacial Lake, also called Guangxieco Lake, developed at the head of Gongzo Glacier. The lake covered an area of 0.42 ± 0.03 km^2 in 1987 (Table 4); however, GPL experienced an outburst on 15 July 1988 (Li and You 1992; Liu et al. 2014). The area of GPL decreased from 0.42 ± 0.03 km^2 in 1987 to 0.19 ± 0.03 km^2 in 1988 after the outburst (Fig. 3). Before 1988, GPL had two outlets, one in the northwestern and another in northeastern part of the lake; however, after the GLOF event on 15 July of 1988, water only

Table 4 Water area and storage of the glacier lakes

Year	Guangxieco Proglacial Lake		Name	New Supraglacial Lake	
	Area ± 1σ (km^2)	Water storage ($\times 10^{-3}$ km^3)		Area ± 1σ (km^2)	Water storage ($\times 10^{-3}$ km^3)
1987	0.42 ± 0.03	21.99 ± 1.88	–	–	
1988	0.19 ± 0.03	10.51 ± 1.90	–	–	–
1995	0.17 ± 0.03	9.48 ± 1.68	–	–	–
2000	0.16 ± 0.03	8.96 ± 1.68	–	–	–
2006	0.21 ± 0.03	11.54 ± 1.81	–	–	–
2009	0.22 ± 0.03	12.05 ± 1.86	–	–	–
			No. 1	0.002 ± 0.002	0.15 ± 0.14
			No. 2	0.008 ± 0.004	0.55 ± 0.26
2013	0.27 ± 0.03	14.58 ± 2.03			
			No. 2	0.013 ± 0.005	0.87 ± 0.37
2017	0.37 ± 0.04	19.55 ± 2.62			
2019	0.43 ± 0.04	22.48 ± 2.55			
			No. 3	0.0029 ± 0.002	0.21 ± 0.15
			No. 4	0.0213 ± 0.006	1.05 ± 0.39

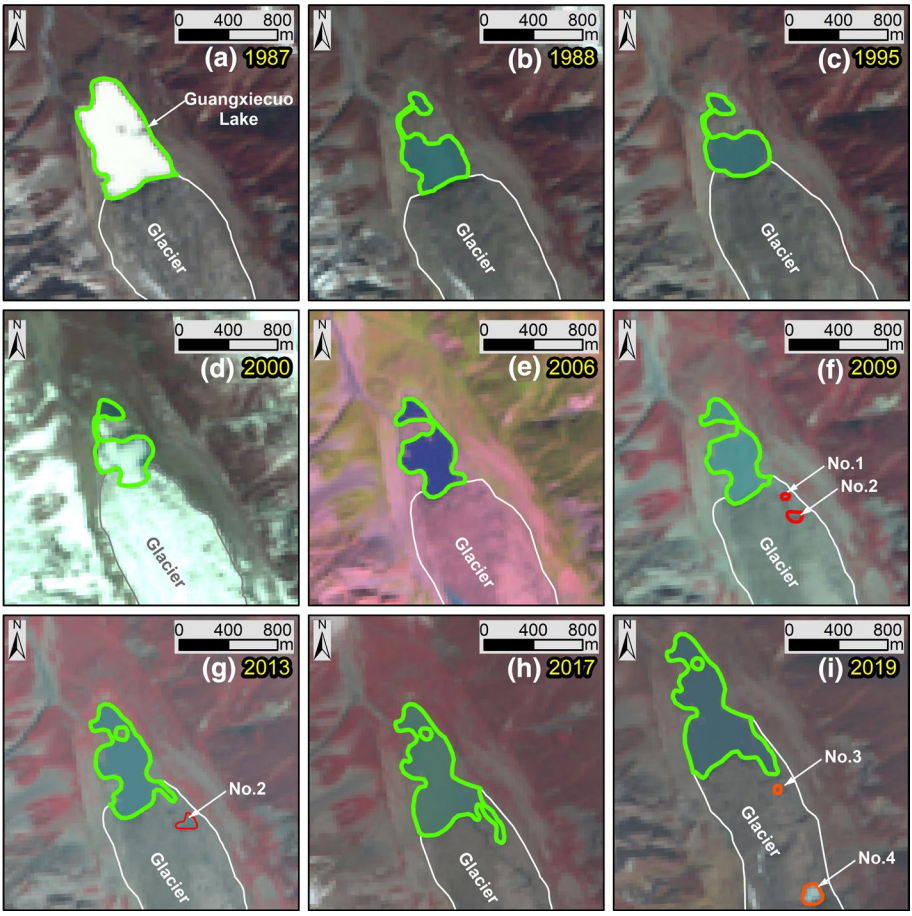

Fig. 3 Evolution of glacial lakes in the study area from 1987 to 2019. Nos. 1 to 4 denote four supraglacial lakes

drained from the northwestern outlet. During the outburst, the lake lost a water volume of 5.40×10^6 m^3. The water area of GPL was divided into two small ponds after this GLOF event, i.e., the North and South glacial lakes. The area of the northern lake was relatively small when compared to that of the Southern lake. The two lakes were joined by a south flowing tributary along with a slope bottom of west lateral moraine (Fig. 3b–d). However, only one water channel formed along with east lateral moraine after ~ 2006 (Fig. 3e).

In addition, two small supraglacial lakes formed on the debris-covered glacier in 2009, identified as lakes No. 1 (with an area of 0.002 ± 0.002 km^2) and No. 2 (0.008 ± 0.004 km^2) (Fig. 3f and Table 4). In 2013, glacial melting along the drainage between lake No. 1 and GPL caused the two to merge. Increased melting in the drainage between supraglacial lake No. 2 and GPL caused these two to merge with a part of the GPL in 2017. By 2019, the area of GPL expanded to an area of 0.43 ± 0.04 km^2, which was larger than the area of GPL in 1987. The water volume of GPL reached $(12.05 \pm 1.86) \times 10^{-3}$ km^3, which also exceeded that of $(21.99 \pm 1.88) \times 10^{-3}$ km^3 in 1987. Meanwhile, two new supraglacial lakes formed on the surface of the

debris-covered glacier, identified as lakes Nos. 3 and 4 with areas of 0.0029 km^2 and 0.0213 km^2, respectively (Fig. 3i and Table 4). The area of GPL has been increasing and also expanding along with the direction of the glacier retreat.

4.3 Climate change

Local climate change has been a critical factor affecting glacier variation as well as the change in the glacial lake in the study area. For example, the meltwater from Gongzo Glacier caused by climate warming was a main source of recharge for GPL. The mean annual air temperature and annual precipitation of three meteorological stations were analyzed to understand their effects on glacier melting and glacial lake evolution. The mean annual air temperatures of Bomi, Zogang, and Zayü stations have increased significantly during the past several decades, with increased slopes of 0.27 °C/decade during the period of 1961–2019 ($p < 0.001$), 0.37 °C/decade during the period of 1978–2019 ($p < 0.001$), and 0.16 °C/decade during the period of 1969–2019 ($p < 0.001$) (Fig. 4a–c). Annual precipitation increased significantly at Bomi station during the period of 1961–2019 with a slope of 3.17 mm/a ($p < 0.05$), while the annual precipitation rates at Zogang and Zayü meteorological stations experienced no significantly increasing trend (Fig. 4d–f).

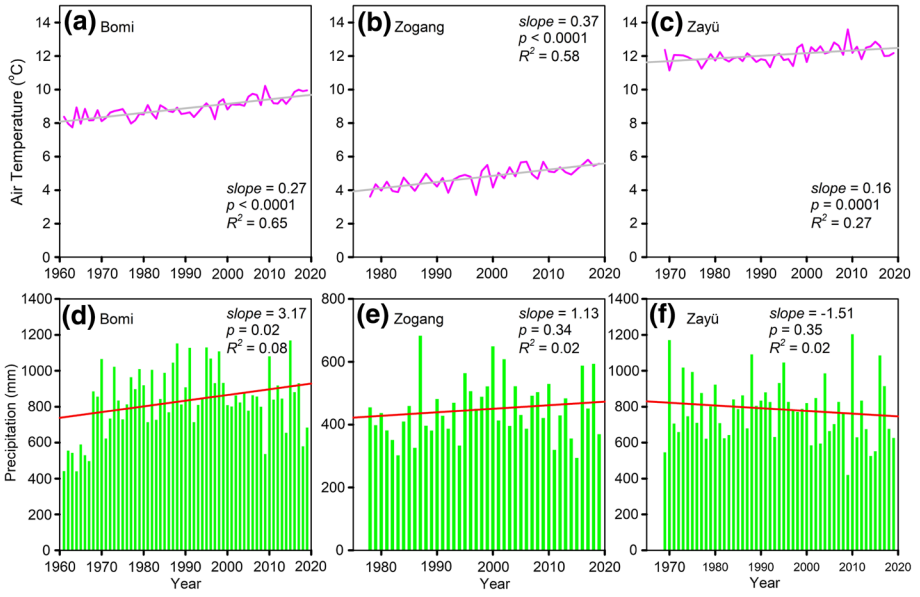

Fig. 4 Changes in mean annual air temperature and annual precipitation at meteorological stations near the Gongzo Glacier, where slope, R^2, and p denote the slope of the regression line (unit: °C/decade or mm/a), determination coefficient, and their level of significance, respectively

5 Discussion

5.1 Changes in monthly mean air temperature and precipitation in 1988

Precipitation from May to October accounted for 71.05%, 92.71%, and 61.45% of the annual total precipitation in Bomi, Zogang, and Zayü, respectively (Fig. 5). In other months, precipitation was mainly concentrated in February–April and fell as snow in this region. The monthly precipitation from February to May in 1988 exceeded the multi-year mean month precipitation at Bomi meteorological station significantly during the period of 1961–1987. Similar increases in monthly precipitation have been found at Zogang and Zayü (except April's precipitation in 1988) meteorological stations. Note that the precipitation in

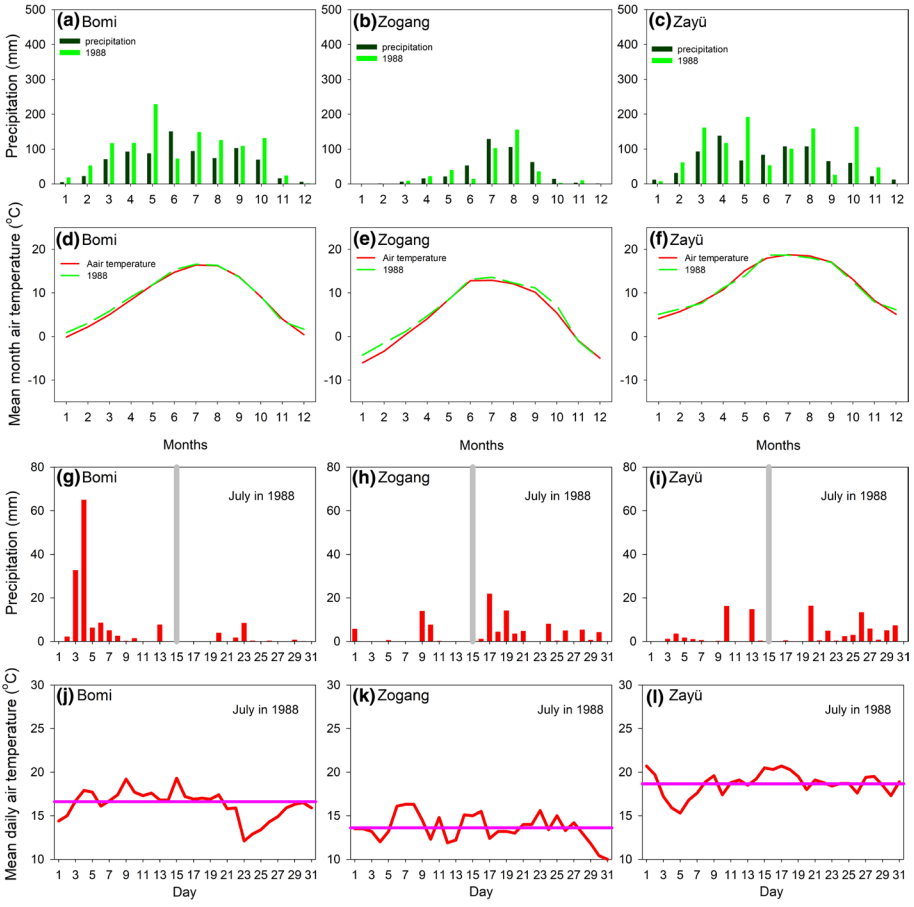

Fig. 5 Changes in monthly air temperature and precipitation at Bomi, Zogang, and Zayü meteorological stations. In plots a–c, black and green bars denote mean monthly precipitation and monthly precipitation in 1988, respectively. In plots d–f, red and green lines denote mean monthly air temperature and monthly air temperature in 1988, respectively. In plots g–i, red vertical bars denote daily precipitation in July 1988. In plots j–l, red and pink lines denote daily air temperature and mean monthly air temperature in July 1988, respectively

June was less than the monthly mean precipitation in multiple years (Fig. 5a–c). Although the precipitation in the week before 15 July 1988 was less than 10 mm per day, heavy daily rainfall events occurred in Bomi on 3 and 4 July 1988 with daily rainfall of 32.8 mm and 65.2 mm, respectively (Fig. 5g). A large volume of rain water was input into the subglacial drainage system.

The monthly mean air temperature during the period of January–August was significantly higher than that of those months in multiple years before 1988 in Bomi and Zogang (Fig. 5d–e). The same situation occurred from January to June in Zayü except for during May (Fig. 5f). In other words, temperature increased progressively in terms of increasing in the water level of GPL due to local rainfall and meltwater from Gongzo Glacier, which partly resulted in the GLOF of the Proglacial Lake (Zhao et al. 2015). A trigger condition is usually needed to stimulate the occurrence of a GLOF event; for example, a glacial surge, earthquake, or a GLOF of a supraglacial lake could trigger a GLOF from a Proglacial Lake. In addition, it was also noted that the monthly air temperature from January to July 1988 was higher than that of those months before 1988, especially the period of January–May, which may often result in a glacial surge. Furthermore, a week before the GLOF event of 1988, daily air temperature in Bomi had remained high. The high air-temperature further accelerated glacial melting and created a large amount of meltwater.

5.2 Changes in the processes of melting and accumulation for Gongzo Glacier

A simple Degree-Day model was used to simulate the mass balance of Gongzo Glacier and understand it during the period of 1961–2019. The annual net mass balance did not change significantly during the period from 1961 to 2019, while the winter and summer mass balances showed significant increasing and decreasing trends, respectively (Fig. 6a). The annual mass balance for 1987–1988 increased. Typically, the winter mass balance for 1987/88 reached a relative maximum, while the high air temperature also resulted in

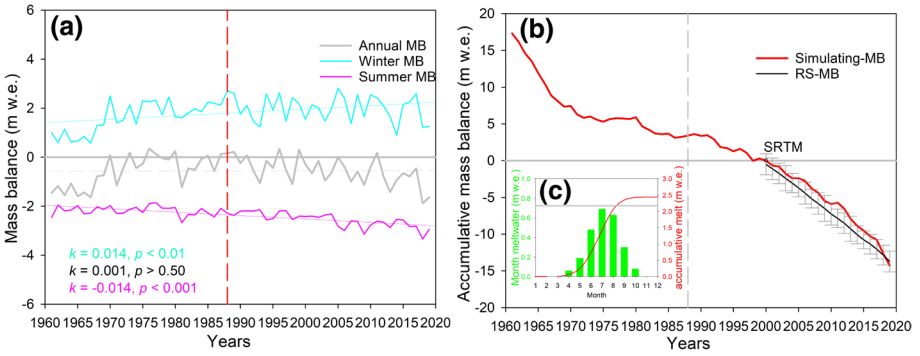

Fig. 6 Simulation of the mass balance (MB) of Gongzo Glacier with a Degree-Day Model using the daily air temperature and precipitation in Bomi meteorological station. (a) Gray, cyan, and pink lines denote the simulated annual net, winter, and summer mass balances, respectively. (b) A red line denotes the accumulative mass balance, which was set as the reference to zero in 2000 to compare the observed mass balance from Remote Sensing (RS). The gray error bar denotes the change of mass balance using RS. (c) Green bars denote the monthly glacier and snow meltwater in 1988; a red line denotes the accumulative meltwater. A horizontal gray line denotes the mean summer meltwater of 2.17 m w.e from 1961 to 1987, i.e., the mean summer mass balance of − 2.17 m w.e

increased glacier melting. In addition, we recognized that a large amount of glacier accumulation in the period had also increased the downward gravity component of the glacier.

The data for the mass balance record of the glacier were acquired beginning in 2000 using Remote Sensing; the SRTM DEM data provide the basal elevation of the glacier surface used to calculate the change in elevation. The modeled accumulative mass balance of the glacier was set to the reference of zero in the year 2000 (SRTM DEM). An important purpose of this conversion was to compare the simulated mass balance and remote sensing measurements. The results showed that the glacier change processes of modeled and actual data from the remote sensing mass balance were very close during the period from 2000 to 2019 (Fig. 6b). That is, the simulation of the glacier mass balance was credible. We also found that the glacier mass has increased continuously since 1987 (Fig. 6b). To further estimate the glacier meltwater in 1988, the rate of glacier melting per month was also simulated (Fig. 6c). Our results showed that the total of glacier and snow melt for April–October was at 2.44 m w.e., which was higher than that of mean summer glacier melt of 2.17 m w.e. during the period of 1961–1987. The total meltwater for April–July was at 1.43 m w.e.; this was especially large with meltwater in July of 0.69 m w.e. These large amounts of glacial meltwater entered into the subglacial drainage system and the glacial lake.

5.3 Evolution of Guangxieco Proglacial Lake

Guangxieco Proglacial Lake was mainly fed by glacial meltwater derived from Gongzo Glacier. The lake was divided into two pools after a GLOF occurred on 15 July 1988 (Liu et al. 2014); the south pond of the glacial lake was directly related to the meltwater from Gongzo Glacier. The only outlet was located in the northwest corner of GPL, while the lake water no longer flowed out from the original outlet located in the northeast corner of the lake. The glacier front was in the lake, which was also affected by an ice avalanche. Some drift ice masses were observed on the surface of the lake (Fig. 7a). The two pools were connected by a water channel along with the bottom of the west lateral moraine and the lake-water flowed between south and north lakes. However, the two small lakes were connected by only one water channel along with east lateral moraine and merged into one lake in 2013 (Fig. 7b). We found that some relatively large lateral moraines existed in the western original channel of the images. These moraines had fallen along with a steep slope of the west lateral moraine because of the effects of freeze–thaw and gravity of the moraines. In fact, the two lakes were connected by an eastern waterway in 2006 (Fig. 3e),

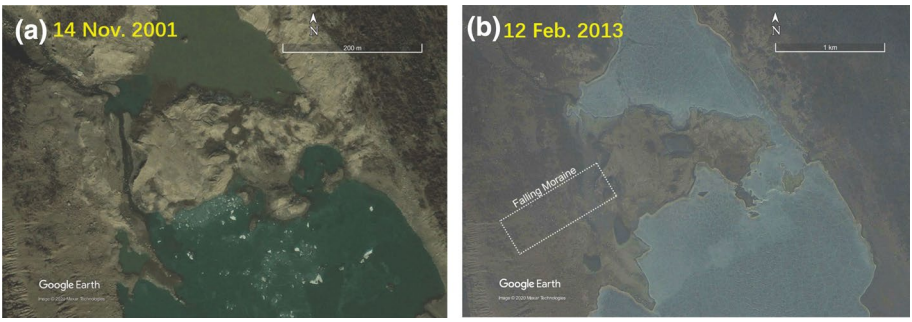

Fig. 7 Changes in the tributary of Guangxieco glacial lake during the period of 2001–2013

while the west water channel was fully blocked by 2009 by the falling moraines, which happened during the period of 2006–2009. Accelerated melting of the glacier caused the lake level to increase so that the region of the western water channel was covered by lake water after 2013. Note that the area of GPL in 2019 was larger than that in 1987, with an increase in lake area of 0.01 km^2 and water storage of 0.49×10^{-3} km^3. It is noted that the calculation of the volume of glacial lake is based on an empirical formula with strong local differences. Our calculation of volume of the glacial lake needs to be calibrated with a field measurement to obtain an accurate result in the later stage. However, this problem does not affect our study of the expansion of the glacial lake and a GLOF event in this paper.

5.4 Formation and disappearance of supraglacial lake

The phenomenon of accelerated glacier melting caused a glacier surface drainage channel to develop in the northeast region of debris-covered glacier front in 2001(Fig. 8). A pit without water was also found in this region. Two supraglacial lakes formed in that region until 2013, identified here as supraglacial lakes Nos. 1 and 2 (Fig. 8b). In fact, the two lakes originally formed in 2009 (Fig. 3f). The water area of lake No. 1 was connected to GPL until they merged into one in 2015. Meanwhile, supraglacial lake No. 2 also expanded during this period (Fig. 8c). During the expansion of lake No. 2 and erosion of the GPL, a water channel formed between GPL and lake No. 2. The glacial lakes Nos. 1 and 2 fully merged into the GPL in 2017 (Fig. 8d). Based on the evolution of the supraglacial lakes Nos. 1 and 2, we deduced that the supraglacial lakes on the water channel of the northeast

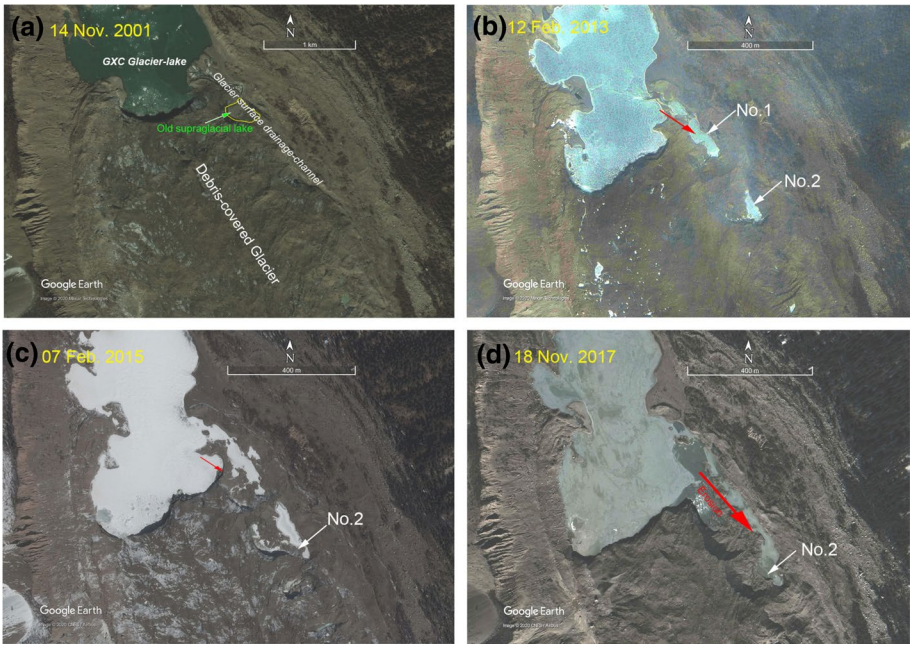

Fig. 8 Expansion of the Guangxieco Proglacial Lake (GPL) and evolution of supraglacial lakes: (a) 14 November 2001, prior to expansion; (b) 12 February 2013, lakes Nos. 1 and 2 form; (c) 07 February 2015, GPL merges with lake No. 1; (d) 18 November 2017, GPL merges with lake No. 2

debris-covered surface resulted from the melting water of the glacier surface and precipitation. The existence of supraglacial lakes accelerated melting of the glacier, which caused the lakes to further expand. Combined with the head erosion of the Proglacial Lake to Gongzo Glacier, the glacier mass loss was further accelerated and GPL finally expanded. Therefore, we found two directions of the GPL expansion, i.e., expanding along with the glacier retreat and within the water channel between GPL and the supraglacial lake.

5.5 Mechanism of the 1988 Gongzo Glacier surge and GLOF

A previous study indicated that the GLOF event that happened on 15 July 1988 resulted from intense pre-precipitation and persistently high temperatures (Liu et al. 2014). An ice avalanche at the glacier terminus in the lake was also a very important factor in terms contributing to the GLOF (Yang et al. 2012). Some ground ice was left in the moraine-dam of the glacier, which contributed to tributaries after the glacier mass loss due to warming air temperatures (Li and You 1992). The GLOF event was accelerated by the tributaries in the glacier dam. These studies described the causes of the GLOF of GPL, but the actual trigger the GLOF event still remains unclear. It was acknowledged that the behavior of the glacial front with connecting to the Proglacial Lake was critical to the expansion of the Proglacial Lake and the GLOF event. A glacial advance is usually a trigger condition in terms of a typical GLOF event.

To understand the conditions that triggered the GLOF, images of the GPL and Gongzo Glacier in June and October in 1988 were analyzed in more detail. The water area of the GPL decreased significantly from 0.427 ± 0.03 km^2 on 05 June to 0.193 ± 0.03 km^2 on 27 October in 1988 (Fig. 9). That is, the GLOF even reduced the water storage capacity by 13×10^{-3} km^3 in the Proglacial Lake. The floods caused by the GPL outburst caused major losses to downstream agriculture, animal husbandry, and villages (Li and You 1992). In addition, we found that the Gongzo Glacier terminus advanced by at least 32.45 m on average from 5 June to 27 October in 1988 (Fig. 9). Glacial meltwater had fed the Proglacial Lake (i.e., GPL), which was a gradual process and did not result in a rapid outburst of the

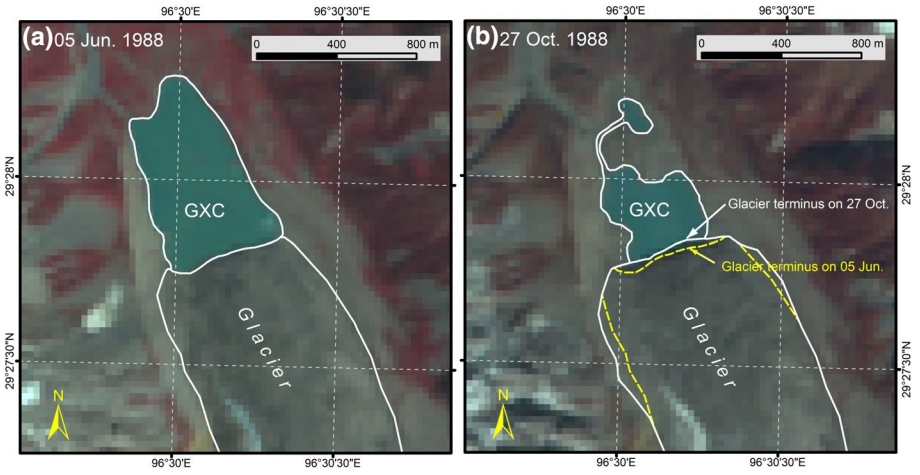

Fig. 9 Glacial advance and the outburst of Guangxieco (GXC) glacial lake (GPL) in 1988: (a) 05 June 1988 remote sensing image, (b) 27 October remote sensing image

Proglacial Lake (Zhao et al. 2015). Glacier advances and supraglacial lake outbursts usually play an important role in a GLOF event (Worni et al. 2012; Stokes and Clark 2003; Fyfe 1990; Sutherland et al. 2020).

The glacier advance/surge played an important role in the GLOF event of 1988. However, several factors cannot be ignored including the periods of heavy rainfall, enhanced melting, and mass input in this glacier. Due to the lack of an on-site record on the GLOF event in 1988, we revisited the glacier front at the end of July in 2021 to clarify the processes involved this GLOF, including observations of the subglacial drainage system and soil properties at the glacial front. Although the information from this survey has not fully represented the glacier background at that time, we believed that the information is helpful in explaining the glacier environment related to the GLOF. Based on the field observations, the subglacial drainage systems were very well developed in the glacial ablation zone (Fig. 10a). Large amounts of clay, silt, and gravel were found in the bottoms of glacial pools (Fig. 10b–d). In particular, this clay and silty sands flowed into the subglacial channel with the mixed meltwater, which was prone to sedimentation in the relative flat channel over time. Over a long period of time, the deposited clay and silty sands would block the subglacial channel (Fig. 10b).

Based on the meteorological records of Bomi station, the precipitation for February–July in 1988 was far greater than that received in previous years (Fig. 5). In particular, the first 2 weeks of July 1988 saw 132.5 mm of precipitation, while the glacier received far more

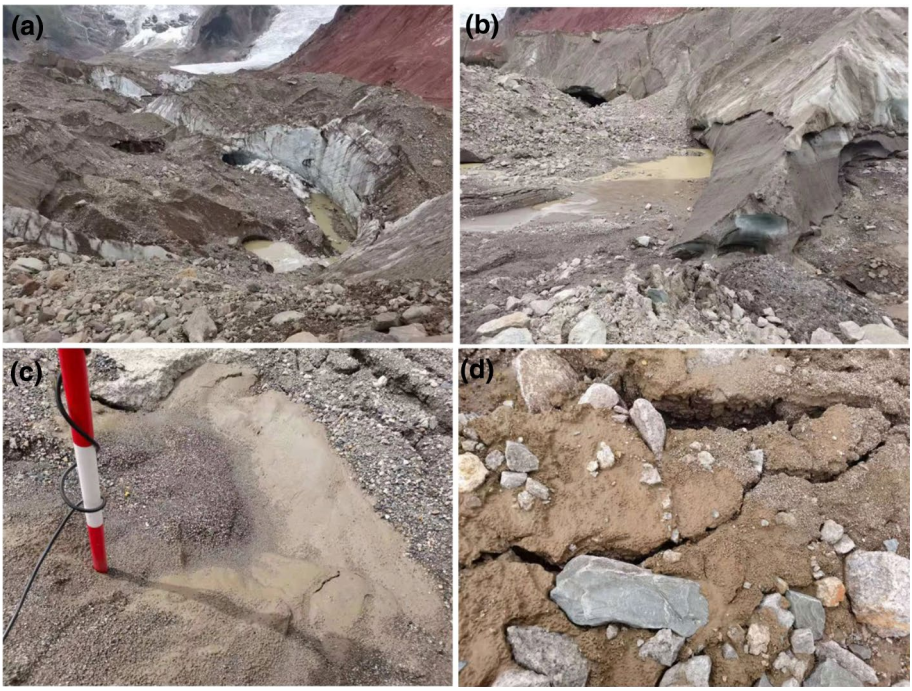

Fig. 10 Photographs of subglacial channels and glacial pool bottom taken on 30 July 2021: **a** subglacial drainage in a large pit after the ice collapsed; **b** a glacial channel in the glacial pool bottom without meltwater; **c** clay, silt, and gravel in the bottom of the subglacial channel; **d** clay and gravel in the bottom of subglacial drainage

precipitation than did Bomi station. At the same time, the glacier meltwater from April to July in 1988 was at 1.43 m w.e., while the meltwater in June and July was at 0.48 m w.e. and 0.69 m w.e., respectively. Both the heavy rainfall and enhanced melting contributed to the water in the subglacial drainage system. The large of rainfall and meltwater was input into the subglacial drainage systems. However, the channel had shrunk or was even blocked by the clay and silty sand sediment. A large volume of water was impounded by the ice wall and elevated the basal water pressure. The mass balance of Gongzo Glacier increased continuously from 1987 to 1989, and the winter mass balance in 1988 was much higher than in the past. That is, a larger glacier mass was locked into the firn snow basin before the melt season in 1988, which significantly increased the downward gravity component of sliding glacier (Kääb et al. 2018; Lei et al. 2021; Cuffey and Paterson 2010). Thus, the glacial advance mainly resulted from the increasing mass balance and the presence of suitable hydrothermal conditions. This glacial advance reopened the subglacial channel, which connected to the terminus. The accumulated subglacial water drained rapidly into the Proglacial Lake and elevated the lake level (Kääb et al. 2018; Imran and Ahmad 2021). Eventually, these conditions led to the GLOF of GPL on 15 July 1988. The trigger factor of the GLOF was the glacial surge in 1988, which was typically hydrologically controlled (Cuffey and Paterson 2010).

5.6 Assessment of the potential GLOF risk

Glacier melt and retreat provided spatial conditions for the expansion of GPL (Carrivick and Tweed 2013). Then, Gongzo Glacier retreated into a deepening glacier basin, while the GPL expanded. The retreating of the glacier front accelerated by calving because of the thermal effects of an expanded glacial lake. This effect caused a further calving-induced retreat and GPL expansion. The positive feedback between the GPL and Gongzo Glacier dynamics was complicated, which has been characterized by the following processes: (i) rapid disintegration of the glacier terminus, or (ii) rapid advances or surges, which reduced the effective pressure at a glacier front margin (Stokes and Clark 2003; Fyfe 1990). Combined with the LandSat images of June and October in 1988, we deduced that the GLOF of GPL on 15 July in 1988 was caused by the surge of Gongzo Glacier (Fig. 8). After that, the Proglacial Lake expanded rapidly due to the increase in glacier meltwater and precipitation. Until 2019, the area of GPL expanded to 0.43 km^2, which exceeded the area of 0.427 km^2 on 05 June in 1988. In addition, new two supraglacial lakes had formed on Gongzo Glacier. In other words, the GPL still showed the potentially high-risk of experiencing a GLOF. The measurements of glacier dynamics and water level of GPL need to be improved in the future. Previous studies have shown that the criteria for determining the nature of potentially dangerous glacial lakes (PDGLs) mainly include a moraine-dammed lake area of more than 0.02 km^2, the rate of lake area increased by more than 20% and the distance between the lake and glacier snout was less than 500 m (McKillop and Clague 2007; Wang et al. 2015; Zhang et al. 2015; Watanabe et al. 2009). Guangxieco Proglacial Lake is a typical PDGL; the lake basin is close to Midui Village and National Highway 318, and its potential risk of experiencing a lake-outburst disaster is very significant. Structural and engineering measures would be required to reduce the lake-surface levels, according to the degree of GLOF impact, with the goal of decreasing pressure on moraine dams and reducing water volume in case of an outburst. Primary techniques and measures for this include controlled breaching, construction of outlet control structures, pumping or

siphoning water from the lake, and tunneling under the moraine dam (Wang et al. 2015; Zhang et al. 2020; Liu et al. 2020; Shugar et al. 2020).

6 Conclusions

Global warming is occurring in the southern Tibetan Plateau where many glaciers are retreating; meanwhile, many glacial lakes have been created and expanded. The water reserves of the glacial lakes often increase as a result of accelerated glacier melting, which has been increasing the risk of GLOF in the glaciated regions. This paper analyzed the cause of the GLOF event at the GPL of Gongzo Glacier on July 15, 1988, and the changes in the glacier during the period of 1987–2019. Based on a series of LandSat TM/ETM + / OLI imagery, we found that the glacier area of Gongzo Glacier decreased by 1.88 km^2 with an APAC of $-5.70 \pm 0.03\%$. The length of the glacial retreat was 0.26 km from 1987 to 2019 with an annual retreat distance of 7.88 m/a. The area of GPL decreased by 0.23 km^2 in 1988, and then, the area again increased until the lake covered an area of 0.43 ± 0.04 km^2 with a water volume of $(22.48 \pm 2.55) \times 10^{-3}$ km^3 in 2019. In addition, four new supraglacial lakes have formed on the glacier surface during the past decade.

The mean annual air temperature around the region has increased significantly in the past several decades, i.e., the increased trend of the mean annual air temperature ranged from 0.16 °C/decade to 0.37 °C/decade. Annual precipitation did not show a significant trend except for at the Bomi meteorological station, where the precipitation had increased significantly.

Based on the remote sensing images of the LandSat TM on 05 June and 27 October in 1988, the front of Gongzo Glacier had advanced by 32.45 m; meanwhile, no significant supraglacial lake was observed on the glacier surface. However, a heavy precipitation event occurred during the first 2 weeks in July 1988 with consistently high daily air temperatures. A large volume of water from rainfall and glacier melting impounded by the ice wall caused an elevation in the basal water pressure. A glacial surge reopened a subglacial tube and the accumulated subglacial water rapidly drained to the GPL. Then, a GLOF event of GPL was triggered by the Gongzo Glacier surge on July 15, 1988.

In addition, we also found that GPL expanded in two main ways. First, the glacier expanded in the direction of the retreating Gongzo Glacier. Second, the glacier expanded by following the glacier meltwater channels between the GPL and this water formed into supraglacial lakes. So far, the latter expansion was more significant than the former. The water volume of GPL in 2019 also exceeded the water reserves in June 1988. The potential risk of a GLOF has been still high, and dynamic monitoring of the GPL and Gongzo Glacier is needed. It is also necessary to strengthen the publicity and popularization of basic knowledge related to disaster prevention and reduction, and enhance the awareness of location residents and land managers of the need for disaster prevention, mitigation, and self-protection.

Authors' contribution YC and SW involved in conceptualization, methodology, writing—original draft, investigation. YW took part in methodology, data curation, visualization, supervision. TP and XM participated in validation, writing—review and editing.

Funding This research was supported by the National Natural Science Foundation of China (Grant No. 42101135), Jiangxi Provincial Natural Science Foundation (Grant No. 20202BAB213013), the Strategic Priority Research Program of the Chinese Academy of Sciences (Grant No. XDA19070503), the projection

of the Environmental Monitoring and Protection in Longhu Mountains of a World Natural Heritage Site from Nanchang Base of the International Centre on Space Technologies for Natural and Cultural Heritage under the Auspices of the United Nations Educational, Scientific, and Cultural Organization (Grant No. HIST-NB), and also supported by the Opening Fund of the Key Laboratory of the Poyang Lake Wetland and Watershed Research (Jiangxi Normal University), Ministry of Education (Grant No. PK2020002).

Declarations

Conflict of interest The authors declare no conflicts of interest.

References

Andreassen LM, Elvehøy H, Kjøllmoen B, Engeset RV (2016) Reanalysis of long-term series of glaciological and geodetic mass balance for 10 Norwegian glaciers. Cryosphere 10:535–552

Carrivick JL, Tweed FS (2013) Proglacial Lakes: character, behaviour and geological importance. Quat Sci Rev 78:34–52

Che Y, Zhang M, Li Z, Wang S, Du M, Wang P, Wang J, Zhou P (2018) Quantitative evaluation of glacier change and its response to climate change in the Chinese Tien Shan. Cold Reg Sci Technol 153:144–155

Cogley JG (2009) Geodetic and direct mass-balance measurements: comparison and joint analysis. Ann Glaciol 50:96–100

Cuffey K, Paterson W (2010) The physics of glaciers. Elsevier, Amsterdam

Ding B, Yang K, Qin J, Wang L, Chen Y, He X (2014) The dependence of precipitation types on surface elevation and meteorological conditions and its parameterization. J Hydrol 513:154–163

Ding M, Huai B, Sun W, Wang Y, Zhang D, Guo X, Zhang T (2018) Surge-type glaciers in Karakoram Mountain and possible catastrophes alongside a portion of the Karakoram Highway. Nat Hazards 90:1017–1020

Ding Y, Liu J (2017) Glacier lake outburst flood disasters in China. Ann Glaciol 16:180–184

Ding Y, Liu S, Li J, Shangguan D (2006) The retreat of glaciers in response to recent climate warming in western China. Ann Glaciol 43:97–105

Emmer A, Cochachin A (2013) The causes and mechanisms of moraine-dammed lake failures in the Cordillera Blanca, North American Cordillera, and Himalayas. Acta Univ Carol Geogr Univ Karlova 48:5–15

Emmer A, Vilímek V (2013) Review Article: Lake and breach hazard assessment for moraine-dammed lakes: an example from the Cordillera Blanca (Peru). Nat Hazards Earth Syst Sci 13:1551–1565

Fyfe GJ (1990) The effect of water depth on ice-proximal glaciolacustrine sedimentation: Salpausselkä I, southern Finland. Boreas 19:147–164

Gilbert A, Flowers GE, Miller GH, Rabus BT, Van Wychen W, Gardner AS, Copland L (2016) Sensitivity of Barnes Ice Cap, Baffin Island, Canada, to climate state and internal dynamics. J Geophys Res Earth Surf 121:1516–1539

Grabs WE, Hanisch J (1992) Objectives and prevention methods for glacier lake outburst moods (GLOFs). Snow Glacier Hydrol 218:341–352

Hall DK, Bayr KJ, Schöner W, Bindschadler RA, Chien JYL (2003) Consideration of the errors inherent in mapping historical glacier positions in Austria from the ground and space (1893–2001). Remote Sens Environ 86:566–577

Hanshaw MN, Bookhagen B (2014) Glacial areas, lake areas, and snow lines from 1975 to 2012: status of the Cordillera Vilcanota, including the Quelccaya Ice Cap, northern central Andes, Peru. Cryosphere 8:359–376

Hugonnet R, Mcnabb R, Berthier E, Menounos B, Nuth C, Girod L, Farinotti D, Huss M, Dussaillant I, Brun F, Kääb A (2021) Accelerated global glacier mass loss in the early twenty-first century. Nature 592:726–731

Imran M, Ahmad U (2021) Geospatially analysing the dynamics of the Khurdopin Glacier surge using multispectral and temporal remote sensing and ground observations. Nat Hazards 108:847–866

Kääb A, Leinss S, Gilbert A, Bühler Y, Gascoin S, Evans SG, Bartelt P, Berthier E, Brun F, Chao W-A, Farinotti D, Gimbert F, Guo W, Huggel C, Kargel JS, Leonard GJ, Tian L, Treichler D, Yao T (2018) Massive collapse of two glaciers in western Tibet in 2016 after surge-like instability. Nat Geosci 11:114–120

Lei Y, Yao T, Tian L, Sheng Y, Wu G (2021) Response of downstream lakes to Aru glacier collapses on the western Tibetan Plateau. Cryosphere 15:199–214
Li DJ, You Y (1992) Bursting of the Midui moraine lake in Bomi, Xizang. J Mt Res 10:219–224
Liu JJ, Cheng ZL, Li Y (2014) The 1988 glacial lake outburst flood in Guangxieco Lake, Tibet China. Nat Hazards Earth Syst Sci 14:3065–3075
Liu Q, Mayer C, Wang X, Nie Y, Wu K, Wei J, Liu S (2020) Interannual flow dynamics driven by frontal retreat of a lake-terminating glacier in the Chinese Central Himalaya. Earth Planet Sci Lett 546:116450
Liu S, Yao X, Guo W, Xu J, Shuangguan D, Wei J, Bao W, Wu L (2015) The contemporary glaciers in China based on the Second Chinese Glacier Inventory. Acta Geogr Sin 70:3–16
Lv RR, Tang BX, Zhu PY (1999) Debris flow and environment in Tibet. Chengdu Science and Technology University Press, Chengdu
Mölg N, Bolch T, Rastner P, Strozzi T, Paul F (2018) A consistent glacier inventory for Karakoram and Pamir derived from Landsat data: distribution of debris cover and mapping challenges. Earth Syst Sci Data 10(4):1807–1827
Mckillop RJ, Clague JJ (2007) Statistical, remote sensing-based approach for estimating the probability of catastrophic drainage from moraine-dammed lakes in southwestern British Columbia. Global Planet Change 56:153–171
Ng F, Liu S, Mavlyudov B, Wang Y (2007) Climatic control on the peak discharge of glacier outburst floods. Geophys Res Lett 34:L21503. https://doi.org/10.1029/2007GL031426
Paul F, Huggel C, Kääb A (2004) Combining satellite multispectral image data and a digital elevation model for mapping debris-covered glaciers. Remote Sens Environ 89:510–518
Paul F, Kääb A, Maisch M, Kellenberger T, Haeberli W (2002) The new remote-sensing-derived Swiss glacier inventory: I. Methods Ann Glaciol 34:355–361
Round V, Leinss S, Huss M, Haemmig C, Hajnsek I (2017) Surge dynamics and lake outbursts of Kyagar Glacier, Karakoram. Cryosphere 11:723–739
Salerno F, Thakuri S, D'agata C, Smiraglia C, Manfredi EC, Viviano G, Tartari G (2012) Glacial lake distribution in the Mount Everest region: uncertainty of measurement and conditions of formation. Global Planet Change 92–93:30–39
Shugar DH, Burr A, Haritashya UK, Kargel JS, Watson CS, Kennedy MC, Bevington AR, Betts RA, Harrison S, Strattman K (2020) Rapid worldwide growth of glacial lakes since 1990. Nat Clim Change 10(10):939–945
Sidjak RW (1999) Glacier mapping of the Illecillewaet icefield, British Columbia, Canada, using Landsat TM and digital elevation data. Int J Remote Sens 20:273–284
Silverio W, Jaquet JM (2005) Glacial cover mapping (1987–1996) of the Cordillera Blanca (Peru) using satellite imagery. Remote Sens Environ 95:342–350
Stokes CR, Clark CD (2003) The Dubawnt Lake palaeo-ice stream: evidence for dynamic ice sheet behaviour on the Canadian Shield and insights regarding the controls on ice-stream location and vigour. Boreas 32:263–279
Sutherland JL, Carrivick JL, Gandy N, Shulmeister J, Quincey DJ, Cornford SL (2020) Proglacial Lakes control glacier geometry and behavior during recession. Geophys Res Lett 47:e2020GL088865
Tiberti R, Buscaglia F, Callieri C, Rogora M, Tartari G, Sommaruga R (2020) Food web complexity of high Mountain Lakes is largely affected by glacial retreat. Ecosystems 23:1093–1106
Veh G, Korup O, Walz A (2020) Hazard from Himalayan glacier lake outburst floods. Proc Natl Acad Sci 117:907–912
Wang S, Che Y, Pang H, Du J, Zhang Z (2020) Accelerated changes of glaciers in the Yulong Snow Mountain, Southeast Qinghai-Tibetan Plateau. Reg Environ Change 20:38
Wang S, Qin D, Xiao C (2015) Moraine-dammed lake distribution and outburst flood risk in the Chinese Himalaya. J Glaciol 61:115
Wang S, Zhang M, Li Z, Wang F, Li H, Li Y, Huang X (2011) Glacier area variation and climate change in the Chinese Tianshan Mountains since 1960. J Geogr Sci 21:263–273
Wang XIN, Chai K, Liu S, Wei J, Jiang Z, Liu Q (2017) Changes of glaciers and glacial lakes implying corridor-barrier effects and climate change in the Hengduan Shan, southeastern Tibetan Plateau. J Glaciol 63:535–542
Watanabe T, Lamsal D, Ives JD (2009) Evaluating the growth characteristics of a glacial lake and its degree of danger of outburst flooding: Imja Glacier, Khumbu Himal Nepal. Norsk Geogr Tidsskr nor J Geogr 63:255–267
Worni R, Stoffel M, Huggel C, Volz C, Casteller A, Luckman B (2012) Analysis and dynamic modeling of a moraine failure and glacier lake outburst flood at Ventisquero Negro, Patagonian Andes (Argentina). J Hydrol 444–445:134–145

Wu K, Shiyin L, Zongli J, Junli X, Junfeng W, Wanqin G (2018) Recent glacier mass balance and area changes in the Kangri Karpo Mountains from DEMs and glacier inventories. Cryosphere 12:103–121
Xu J, Liu S, Guo W, Zhang Z, Wei J, Feng T (2015) Glacial Area changes in the Ili River Catchment (Northeastern Tian Shan) in Xinjiang, China, from the 1960s to 2009. Adv Meteorol 2015:12
Yang R, Zhu L, Wang Y, Chu D (2012) Study on the variations of Lake Area and volume and their effect on the occurrence of outburst of MUDUI Glacier Lake in Southeastern Tibet. Prog Geogr 31:1133–1140
Yao X, Liu S, Wei J (2010) Reservoir capacity calculation and variation of Moraine-dammed Lakes in the North Himalayas: a case study of Longbasaba Lake. Acta Geogr Sin 65:1381–1390
Zhang G, Yao T, Xie H, Wang W, Yang W (2015) An inventory of glacial lakes in the third pole region and their changes in response to global warming. Global Planet Change 131:148–157
Zhang G, Yao T, Xie H, Yang K, Zhu L, Shum CK, Bolch T, Yi S, Allen S, Jiang L, Chen W, Ke C (2020) Response of Tibetan Plateau lakes to climate change: trends, patterns, and mechanisms. Earth Sci Rev 208:103269
Zhang Y, Liu S, Ding Y (2017) Observed degree-day factors and their spatial variation on glaciers in western China. Ann Glaciol 43:301–306
Zhao W, Chen X, Liu J, Su F (2015) Outburst-regeneration characteristic and mechanism of Glacier Lake. Mt Res 33:703–712
Zheng G, Allen SK, Bao A, Ballesteros-Cánovas JA, Huss M, Zhang G, Li J, Yuan Y, Jiang L, Yu T, Chen W, Stoffel M (2021) Increasing risk of glacial lake outburst floods from future Third Pole deglaciation. Nat Clim Chang 11:411–417